RESEARCH ARTICLE
doi: 10.2306/scienceasia1513-1874.2024.070

ScienceAsia 50 (3): 2024: ID 2024070: **1–10**

Cell adhesion molecule 2 inhibits colorectal cancer progression through attenuating epithelial-mesenchymal transition

Yangyang Liu[a,†], Daoquan Fang[a,†], Xiaojuan Fang[b,†], Zuyue Zhong[a], Qiongying Zhang[e], Yichu Lian[f], Fanggui Shao[c,d,*], Lei Jiang[a,f,*]

[a] Central Laboratory, The First Affiliated Hospital of Wenzhou Medical University, Zhejiang 325000 China
[b] Key Laboratory of Intelligent Treatment and Life Support for Critical Diseases of Zhejiang Province, The First Affiliated Hospital of Wenzhou Medical University, Zhejiang 325000 China
[c] Department of Laboratory Medicine, the First Affiliated Hospital of Wenzhou Medical University, Zhejiang 325000 China
[d] Department of Clinical Laboratory, Key Laboratory of Clinical Laboratory Diagnosis and Translational Research of Zhejiang Province, the First Affiliated Hospital of Wenzhou Medical University, Zhejiang 325000 China
[e] Department of pathology, the First Affiliated Hospital of Wenzhou Medical University, Zhejiang 325000 China
[f] Cixi Biomedical Research Institute, Wenzhou Medical University, Zhejiang 315000 China

*Corresponding authors, e-mail: fangguishao@wmu.edu.cn, lei.jiang@wmu.edu.cn
† These authors contributed equally to this work.

Received 11 Oct 2023, Accepted 22 May 2024
Available online 21 Jul 2024

ABSTRACT: Analysis of colorectal cancer (CRC) data revealed that cell adhesion molecule 2 (CADM2) is lowly expressed in tumor tissues. This study, therefore, aimed to elucidate the anti-oncogenesis roles of CADM2. The expression level CADM2 in The Cancer Genome Atlas (TCGA) were analyzed. We validated the expression level in adjacent normal, tumor, and metastatic tissues through real-time polymerase chain reaction (PCR) and immunohistochemistry (IHC). Methylation-specific PCR was used to explore the reason for the low expression. The biological function of CADM2 was verified by analyzing CCK-8 and transwell in cell line. Bioinformatics and Western blot analyses were used to explore anti-tumor progression pathways and the differences in immune infiltration levels. We found that CADM2 is weakly expressed in the TCGA and has good diagnostic performance. The low expression of CADM2 in cell lines and tissues was confirmed, and the hypoexpression was correlated with promoter hypermethylation. The IHC showed statistically significant decreased expression in primary focal compared to adjacent normal tissue, which further reduced in metastatic foci compared with primary foci. Up-regulation of CADM2 inhibited the growth and migrative and invasive ability of cells. When CADM2 expression was up-regulated, significant changes occurred in the expression of epithelial-mesenchymal transition (EMT)-related protein. Bioinformatics analysis indicated that the molecular mechanism of CADM2 inhibiting tumor progression may also be related to the EMT process. Moreover, the CADM2 high-expression subgroup had higher immunity scores and infiltration levels. The research showed the association of CADM2 with carcinogenesis and metastasis by EMT process, providing new insight for molecular therapy and diagnosis of CRC.

KEYWORDS: colorectal cancer, progression, CADM2, epithelial-mesenchymal transition

INTRODUCTION

Colorectal cancer (CRC) is the third leading cause of cancer death worldwide with more than 1.85 million cases and 850,000 deaths per year [1, 2]. Of those newly diagnosed CRC, approximately 35% of patients have metastatic disease at diagnosis, and another 50% presenting with localized disease will eventually have metastatic disease. Approximately 70–75% of patients diagnosed with metastatic CRC disease survive more than 1 year, 30–35% survive more than 3 years, and less than 14% survive more than 5 years [2–4]. Studies have shown that genes, proteins, mutations, and non-coding RNAs play important roles in tumor development and may provide new insights for molecular therapy of CRC [5–8].

CADMs belong to the immunoglobulin superfamily and include CADM1, CADM2, CADM3, and CADM4, which are characterized by 3 extracellular Ig-like loops, a transmembrane region, and an intracellular domain. CADMs are mainly involved in binding cells with other cells or with the extracellular matrix (ECM) and are crucial components in the maintenance of tissue structure and function [9–11]. Studies have confirmed that CADM2 is associated with obesity [12], diabetes [13], psoriasis [14], pulmonary injury [15], and stroke [16]. Recently, an increasing number of findings have shown that CADM2 plays a crucial role in carcinogenesis. For example, a retrospective analysis showed that low CADM2 expression predicts a high risk of recurrence in hepatocellular carcinoma after hepatectomy [17]. Moreover, CADM2 may inhibit proliferation, migration, and invasion of clear cell renal cancer through hypoxia-mediated regulation [18]. Down-regulation of microRNA-182 inhibits cell viability, invasion, and angiogenesis in retinoblastoma through inhibition of

the PI3K/AKT pathway and CADM2 up-regulation [19]. Although researchers have recently reported that CADM2 plays an anti-oncogenic role in colon cancer cells, the mechanism of its anti-carcinogenesis has not been reported, and the correlation between its expression level and clinical features has not been elucidated [20].

The immune cell composition within colorectal cancer tumors is heterogeneous with immune cell subgroups located at the core or invasive margins of the tumor, directly interacting with malignant cells [21]. Extensive research has shown that T cells exhibit important anti-tumor activity and play a crucial role in tumor control. Increased expression of genes encoding components of the Th1 pathway and CD8 T cells has been observed in colorectal cancer tumors, which show no early signs of metastasis compared to tumors of this nature [22]. Furthermore, the expression of these genes is negatively correlated with tumor recurrence. Extensive intratumoral infiltration of NK cells has a favorable prognostic impact on colorectal cancer [23].

In our study, low expression of CADM2 in CRC was detected in CRC by analyzing The Cancer Genome Atlas (TCGA) databases and validated at the mRNA and protein levels using cell lines and clinical samples. A large number of samples were tested to verify the clinical usefulness of CADM2 as a biomarker and the expression level of CADM2 in primary and metastatic foci. The cell biological function of CADM2 and the pathway to inhibit tumor metastasis were further explored. In addition, we analyzed the differences in immune infiltration levels and immune scores among different CADM2 expression level subgroups.

METHODS

Patients enrolled

Paraffin-embedded tissue samples (59 of adjacent normal and 467 of CRC tissue from 454 patients) were collected from the First Affiliated Hospital of Wenzhou Medical University. Of the 454 patients, 45 had paired adjacent normal and tumor tissues. Of the 45 patients, 12 had paired adjacent normal, tumor, and metastatic tissues. Thirty paired adjacent normal and tumor fresh tissues were collected from patients who underwent colorectal tumor resection. The diagnosis of CRC was confirmed by experienced pathologists based on histological evidence. This study was approved by the Ethics Committee of the First Affiliated Hospital of Wenzhou Medical University (KY2022-R210).

Data mining

First, mRNA data of 41 normal and 480 tumor tissues were obtained from TCGA database to verify the expression of CADM2 in CRC. Subsequent experimental verification involved differential mRNA expression of CADM2 in cell lines and selected 30 paired CRC samples. The protein level of CADM2 was detected by immunohistochemistry (IHC) in 59 adjacent normal tissues and 467 tumor samples.

RNA extraction, reverse transcription, and quantitative PCR (RT-qPCR)

Total RNA from cell lines and tissues was extracted using TRIzol Reagent (Thermo Fisher Scientific, USA) according to the manufacturer's instructions. Total RNA (500 ng) was reverse-transcribed to cDNA using a PrimeScript RT Reagent Kit (TaKaRa, China). The cDNAs were then amplified for qPCR using SYBR Green (TaKaRa) and analyzed by ABI QuantStudio5 (Thermo Fisher Scientific). The primers used for qPCR were summarized in Table S1.

Methylation-specific PCR analysis

Genomic DNA from 30 paired adjacent normal and tumor tissues was extracted using the QIAcube automated DNA extraction system (Qiagen, Germany) according to the manufacturer's instructions. One μg genomic DNA was modified by sodium bisulfite using the EZ DNA methylation™ kit (Zymo, USA). Modified genomic DNA was amplified with specific primer sets using SYBR Green Mix (TaKaRa). The exact position of the CpG site used for methylation-specific PCR analysis in our experiments was the CADM2 5′-untranslated region from - 442 to - 659, for which we designed primers and performed amplification analysis. The primers used for methylation-specific PCR were also summarized in Table S1. The two-step reaction conditions were 95 °C for 30 s, 40 cycles of 95 °C for 5 s, and 60 °C for 60 s. Finally, the relative methylation level for each sample was normalized to the control ACTB expression and calculated by the ΔCt.

Immunohistochemical staining

The tissues were fixed, dehydrated, embedded, and sectioned (3.5 μm). The slides were stained with anti-CADM2 antibody (#34182, 1:500, Signalway Antibody, USA). Images were acquired using a microscope (DP80, Olympus, Japan). Staining results were independently assessed by 2 pathologists. The score adopts the H-Score (Histochemistry score) histological scoring system, H-SCORE $= \sum(\text{pi} \times \text{i}) =$ (percentage of weak intensity × 1) + (percentage of moderate intensity × 2) + (percentage of strong intensity × 3), where pi represents the pixel area of the positive cell number ratio, and i represents staining intensity. The H-score ranges from 0–300; the larger the score, the stronger the comprehensive positive intensity.

Cell culture and lentiviral vector

Cell lines FHC, HT-29, SW620, DLD-1, SW480, and CaCo2 were purchased from the Cell Bank of the Chinese Academy of Sciences (China), cultured in RPMI 1640/DMEM medium containing 10% fetal bovine serum (FBS), and incubated at 37 °C in a 5% CO_2

incubator. Full-length CADM2 DNA fragments were amplified by PCR and cloned into pCDH-GFP-Puro vector (Ruibo, China), and lentivirus was produced using packaging plasmids pCMV-VSVG, pMDLg/pRRE, and pRSV-REV in our laboratory, as previously described [24].

Cell counting kit-8 (CCK-8) assay

Cell growth was determined by the CCK-8 assay (Dojondo Laboratories, Japan). Briefly, 5,000 cells per well were seeded in 96-well plate, and 10 µl of CCK-8 solution was added to each well at the indicated time points and incubated for 3 h. Absorbance at 450 nm was measured using a microplate reader.

Colony formation assay

Cell lines (DLD-1 and SW480) were seeded in 6-well plate (Corning, USA) at 500 cells/well. Plates were then incubated for 14 days under standard culture conditions, stained with 0.1% crystal violet (Beyotime, China) for 0.5 h, imaged under a microscope (Olympus), and archived.

Transwell assays

For migration assay, a 24-well plate (Corning) with an 8 µm pore polycarbonate membrane was used. Then, 1×10^5 cells were seeded into the upper chamber, and 200 µl of serum-free RPMI-1640 was added. For invasion assay, the procedure was the same as migration assay, except that the matrix gel needs to be laid down in the pore polycarbonate membrane in advance. subsequently, the membrane was stained with crystal violet and photographed for counting. The number of migrating and invasive cells was counted in 3 randomly selected fields.

Real-time cell analysis

Real-time cell analysis was performed using a modified 16-well plate (Agilent Technologies, USA), with each well consisting of upper and lower chambers separated by a microporous membrane with randomly distributed 8 µm pores. This setup is analogous to the traditional Transwell plate with microelectrodes attached to the bottom of the membrane for impedance-based migration cell detection. For Real-Time Cell Analysis (RTCA), 30 µl serum-free RPMI-1640 was added to the upper chamber, and 165 µl of 20% serum RPMI-1640 was added to the lower chamber and equilibrated in a 37 °C, 5% CO_2 cell culture incubator for 1 h. After that, baseline measurement was performed using the xCELLigence RTCA DP Analyzer (Agilent Technologies). Subsequently, cells were seeded in the upper chamber of each well, and the plate was placed in the RTCA Station inside the incubator. The scanning was performed every 15 min for a total of 24 h. The invasion experiment is similar to the migration experiment, except that a matrix gel needs to be pre-coated on a porous polycarbonate membrane in advance and scanned every 15 min for a total of 48 h.

Western blot analysis

Cells were lysed with RIPA lysis buffer (Thermo Fisher Scientific) containing protease inhibitors (Sigma-Aldrich, Germany). Protein concentrations were quantified using the BCA analysis kit (Sigma-Aldrich). Proteins were then electrophoresed in a polyacrylamide gel and transferred to a PVDF membrane. Primary antibody was added to the proteins overnight at 4 °C. The next day, the secondary antibody was incubated with the protein for 1 h at room temperature. ECL Western Blotting Substrate (Thermo Fisher Scientific) was used to detect protein bands on a Gel Doc XR + system (Bio-Rad, CA, USA). The following primary antibodies were used: CADM2 (#34182, 1:1000); GAPDH (AF7021, 1:5000, Affinity Biosciences, USA); E-cadherin (#3195 1:1000) and Vimentin (#5741, 1:1000) from Cell Signaling Technology, USA); and Slug (#ab27568, 1:1000, Abcam, UK).

Immune infiltration

Data for immune infiltration analysis were obtained from the TCGA database, RNAseq data in FPKM (Fregments per Kilobase per Million) format were log2 transformed for subsequent analysis, and markers for 24 immune cells were obtained from the literature [25].

Bioinformatics analysis

Genomic data of 41 normal and 480 tumor tissues were obtained from the TCGA database (https://portal.gdc.cancer.gov). The correlation between CADM2 expression and promoter methylation level was analyzed based on Illumina 450 methylation data from the TCGA database. The predictive effect of CADM2 expression levels was evaluated by the "pROC" package of the R software using a combination of accuracy, sensitivity, specificity, and area under the receiver operating characteristic (ROC) curve. The "ggplot" package was used to visualize single-gene co-expression, correlation heat maps, and scatter plots between CADM2 and epithelial-mesenchymal transition (EMT)-related proteins. The correlation between CADM2 expression level and immune infiltration was determined by the GSVA package and ssGSEA algorithms of R software.

Statistical analysis

Data are presented as mean ± standard deviation (SD). Enumeration data were compared using the chi-square test, and continuous data were compared with an independent *t*-test (SPSS 23.0, USA). Spearman's rank correlation served as a measure for evaluating the correlation. A *p*-value of less than 0.05 was considered statistically significant (ns, not significant; *, $p < 0.05$; **, $p < 0.01$; ***, $p < 0.001$; and ****, $p < 0.0001$).

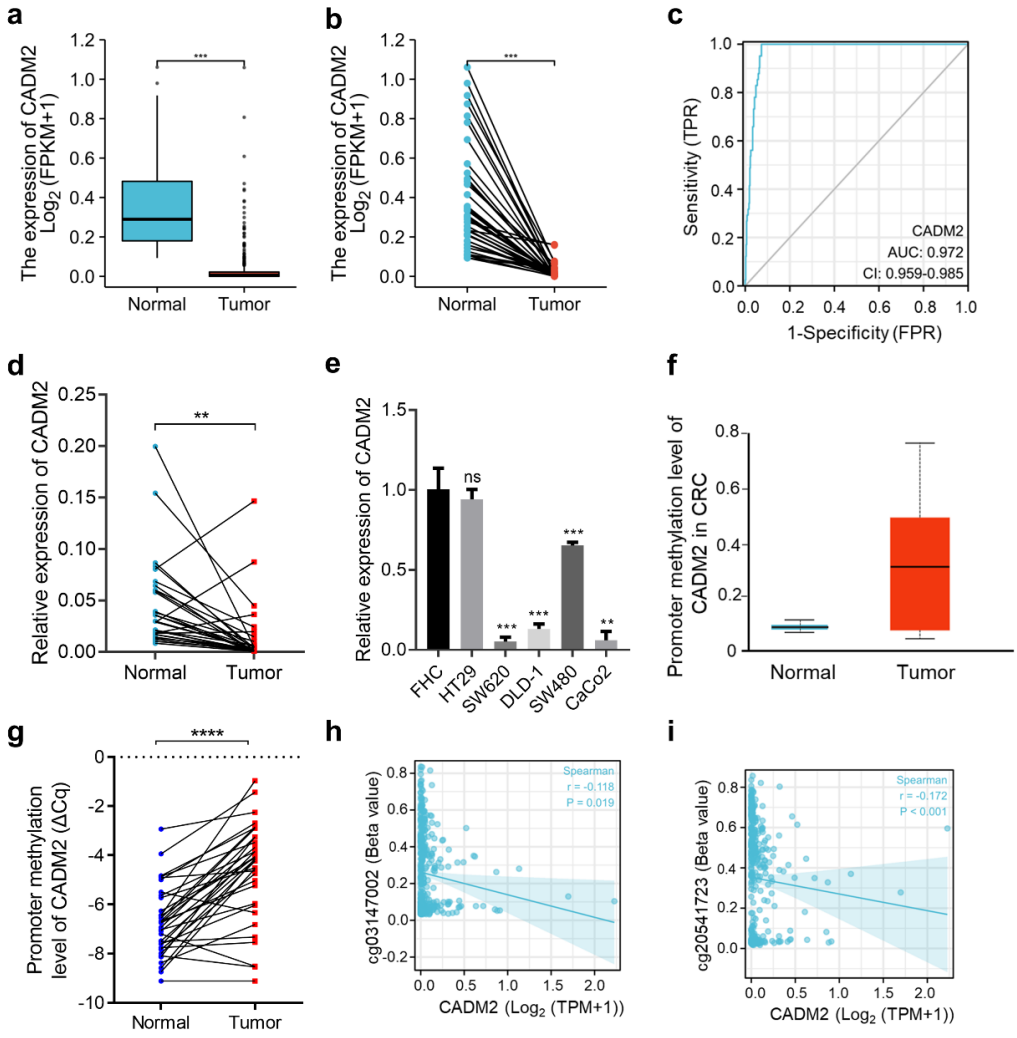

Fig. 1 The level of mRNA expression and promoter methylation of CADM2 in colorectal cancer (CRC) tissue. Unpaired (a) and paired (b) analysis of mRNA expression of CADM2 in normal and tumor tissues based on The Cancer Genome Atlas (TCGA) data. (c) Receiver operating characteristic curves of CADM2 mRNA expression levels. (d) The mRNA expression of CADM2 determined by real-time PCR in paired CRC tissues ($n = 30$). (e) The mRNA expression of CADM2 in intestinal epithelial cell line FHC and CRC cell lines. (f) The promoter overall methylation level of CADM2 in unpaired CRC tissues. (g) Methylation-specific PCR analysis of the promoter methylation level of CADM2 in paired CRC tissues ($n = 30$.) (h–i) The correlation between CADM2 expression level and specific location promoter methylation level. ns, no significance; *, $p < 0.05$; **, $p < 0.01$; ***, $p < 0.001$; and ****, $p < 0.0001$.

RESULTS

The mRNA expression of CADM2 down-regulated in CRC

Analysis of expression data from the TCGA database showed that CADM2 exhibited low expression in tumor tissues from unpaired and paired CRC samples (Fig. 1a,b). Predicting the outcome based on CADM2 expression, the mean expression levels in the normal ($n = 41$) and tumor ($n = 480$) groups were 0.829 ± 0.53 and 0.081 ± 0.206, respectively. CADM2 had high performance in the diagnosis of CRC when the cut-off was 0.218 (Area under Curve (AUC) = 0.972, CI = 0.959–0.985) (Fig. 1c). Examination of mRNA in the selected 30 pairs of adjacent normal and tumor tissues from our cohort revealed that CADM2 mRNA expression was also down-regulated in tumor tissues (Fig. 1d). Similarly, the mRNA expression of CADM2 was lower in CRC cells compared with normal human intestinal epithelial cell line FHC (Fig. 1e).

Hypoexpression of CADM2 caused by methylation of the promoter

Previous studies have shown that loss of heterozygosity (LOH), mutations, and gene promoter methylation contribute to the inactivation of tumor suppressor genes in cancer [26]. We found that the higher overall promoter methylation of CADM2 in the UALCAN database (Fig. 1f) was experimentally confirmed in tumor tissues from 30 paired CRC tissues (Fig. 1g). Since we only collected paired fresh tissues of colorectal cancer and adjacent non-cancerous tissues, but not fresh tissues from metastatic lesions, we were unable to assess the methylation level of CADM2 in metastatic lesions. Subsequently, we tested the correlation between the methylation level of 10 CpG sites and the expression level of CADM2 from TCGA Illumina 450 methylation data. These 2 sites (cg03147002 and cg20541723) in the manuscript are representative and can reflect a negative correlation between CADM2 expression levels and methylation levels in the promoter region (Fig. 1h,i). The methylation levels of 3 out of the remaining 8 CpG sites (cg03416562, cg22380921, and cg15355387) are also negatively correlated with the expression levels of CADM2 and are statistically significant; the 5 out of 8 CpG site are negatively correlated but not statistically significant. The scatter plot of the correlation for these 8 sites has been placed in Fig. S1. This suggests that the hypoexpression of CADM2 may be caused by the hypermethylation of the promoter.

Low protein expression of CADM2 in primary and metastatic CRC

We examined CADM2 protein expression by IHC in 59 adjacent normal and 467 tumor tissues. Representative staining for CADM2 is shown in Fig. 2a; the results showed that the expression of CADM2 was significantly lower in tumor tissues than that in normal tissues ($p < 0.0001$) (Fig. 2b). In 45 patients who had paired normal and tumor tissues, CADM2 expression was statistically significant lower in the primary foci compared with normal tissues ($p < 0.0001$) (Fig. 2c). In 12 patients who had paired normal, primary tumor, and metastatic tissue, CADM2 expression was also lower in normal tissue than that in primary tumor and further decreased in the metastatic lesions compared with the primary lesions (Fig. 2d).

Overexpression of CADM2 inhibiting cell growth, migration, and invasion in CRC cells

We overexpressed CADM2 in DLD-1 and SW480 cell lines, and the up-regulation of CADM2 expression was verified by Western blot analysis (Fig. 3a,b). As shown in Fig. 3c,d, up-regulation of CADM2 significantly inhibited cell growth. The migrative and invasive ability of CRC cells was drastically reduced (Fig. 3e,f). Furthermore, by utilizing RTCA to further analyze cell migration and invasion, it is indeed observed that overexpression of CADM2 significantly inhibits the rate of cell migration and invasion (Fig. 3g).

CADM2 inhibiting EMT process in CRC

CADM2 expression was lower in primary foci and further decreased in metastatic foci. To elucidate its role in the metastatic process, we detected EMT pathway-related proteins expressions by Western blot analysis. Overexpression of CADM2 increased the expression of E-cadherin and decreased the expression of vimentin and Slug, suggesting that EMT is involved in this progression process (Fig. 4a,b). We then performed correlation analysis for CADM2, and the results showed that CADM2 was significantly correlated with proteins involved in the EMT process, including ZEB1, ZEB2, PDGFB, PAK1, ZO-1, LIMK, SMAD3, SMAD4, FN, SMAD2, SNAIL2, and MMP2. Among them, CADM2 was negatively correlated with PAK1 and LIMK and positively correlated with the remaining proteins (Fig. 4c–e).

Relative abundance of CADM2 in immune infiltration

The correlation between CADM2 expression and the extent of immune cell infiltration in CRC tissues was analyzed. High CADM2 expression was significantly positively correlated with activated DC (aDC), cytotoxic cells, T helper cells, T cells, Th1 cells, neutrophils, Treg, T central memory (Tcm), T gamma delta (Tgd), plasmacytoid DC (pDC), T effector memory (Tem), DC, T follicular helper (Tfh), NK cells, immature DC (iDC), B cells, macrophages, eosinophils, and mast cells in CRC, and the enrichment scores of immune cells were higher. This indicates that immune cells are active when it is highly expressed (Fig. 5).

DISCUSSION

CADM2 is a member of the adhesion molecule family and interacts homophilically and heterophilically with other CADM family members, leading to cell aggregation and the organization of functional synapses through heterophilic adhesion. In recent years, its anti-oncogenesis effect has been noted by researchers. Li et al [27] found that CADM2 is lowly expressed in esophageal squamous cell carcinoma (ESCC) and that up-regulation can inhibit cell proliferation and induce apoptosis in ESCC cells. In renal cell carcinoma [28] and prostate cancer [10], CADM2 also acts as a tumor suppressor, and low CADM2 expression in patients with hepatocellular carcinoma predicts a higher risk of recurrence after hepatectomy [17]. Moreover, miR-146a regulated by hypoxia targets CADM2 to promote proliferation, migration, and invasion of clear cell renal cell carcinoma [18]. We found for the first time that the expression level of CADM2 was lower in CRC metastatic foci than that in primary foci. However,

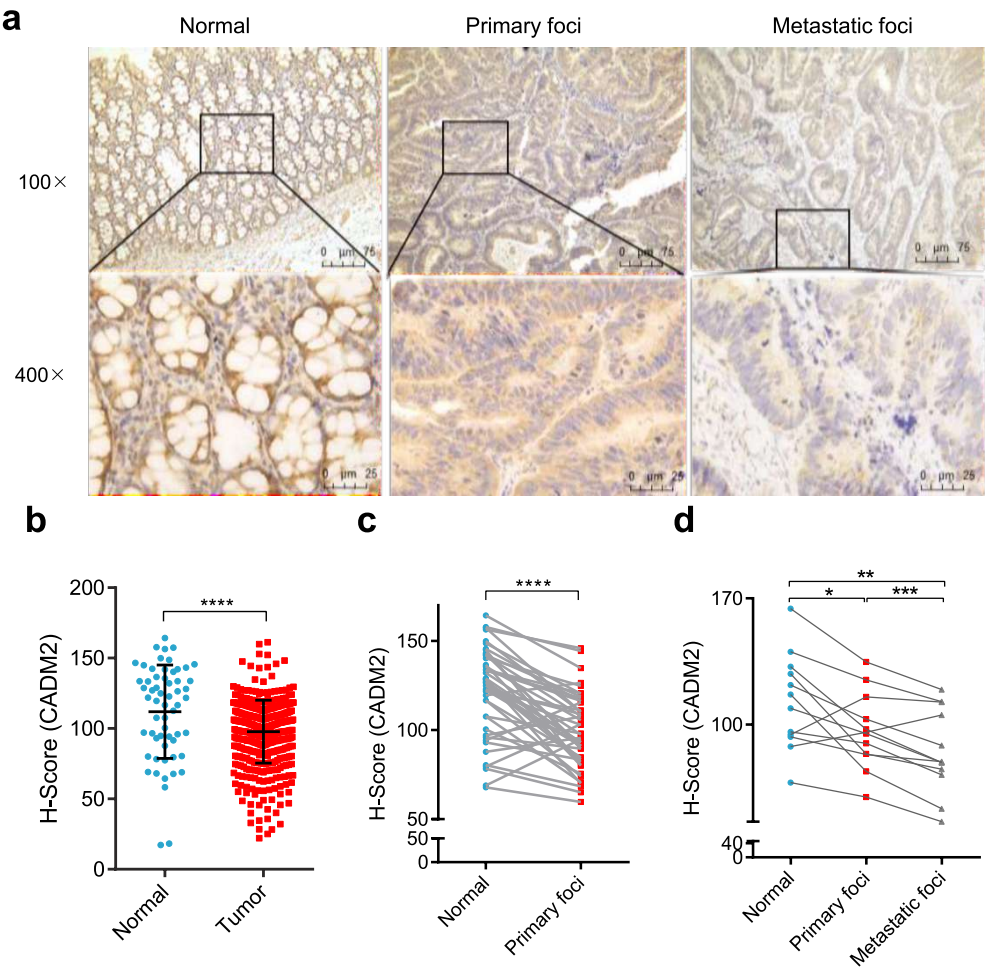

Fig. 2 CADM2 protein expression in primary and metastatic foci. (a) Immunohistochemistry (IHC) analysis of CADM2 protein expression in colorectal cancer (CRC) tissue. (b) CADM2 protein expression determined by IHC in 59 normal and 467 tumor tissues. (c) CADM2 protein expression in 45 paired CRC tissue and adjacent normal tissue samples. (d) CADM2 protein expression in 12 patients with paired normal, primary tumor, and metastatic tumor tissues.

Dai et al [29] considered that CADM2 might be a poor prognostic factor in patients with brain metastasis of NSCLC, which was up-regulated in patients with brain metastasis of NSCLC compared to patients without brain metastasis. Since our colorectal cancer metastatic tissues were mainly liver and lung, which are completely different from NSCLC metastasis to the brain, we speculate that CADM2 plays different pro-metastatic roles in different cancer types. Currently, the prognostic or predictive value for CRC is unknown. In this study, we found for the first time that CADM2 was used as a biomarker for CRC and showed high diagnostic efficiency (AUC = 0.972, CI = 0.959–0.985).

Methylation, a common epigenetic modification, can inactivate tumor suppressor oncogenes, and many tumor suppressor genes undergo CpG hypermethylation and subsequent loss of expression, such as the APC [30], CD44 [31] and CDH1 [32]. CADM2 is no exception. Chang et al [10] confirmed that hypoexpression of CADM2 correlates with promoter hypermethylation in prostate cancer. He et al [28] confirmed that aberrant methylation and loss of expression of the tumor suppressor CADM2 are associated with tumor progression in human renal cell carcinoma. The RHEB methylation is a new highly sensitive and specific tumor marker from DNA methylation change in white blood cells of breast cancer patient blood and may be considered a tumor marker for breast cancer screening [33]. In the present study, we demonstrated that CADM2 expression was also reduced by promoter methylation and that the methylation level was negatively correlated with the expression level in CRC.

Metastasis is a multi-step process in which tumor cells spread from the primary foci and form secondary tumors at a distant location. The IHC results of CADM2 showed statistically significant decreased expression in

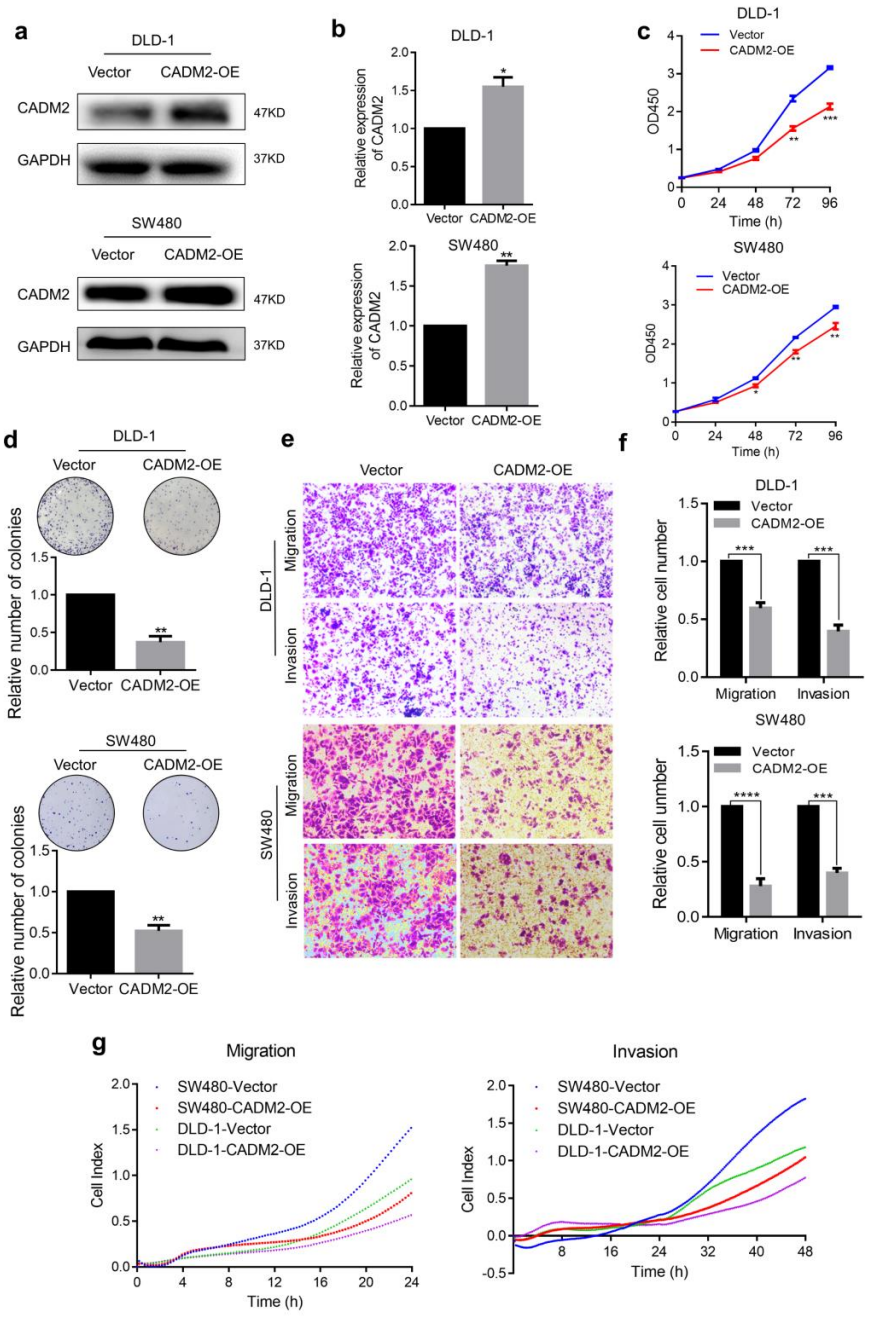

Fig. 3 Overexpression of CADM2 inhibiting growth, migration, and invasion in colorectal cancer (CRC) cells. (a–b) The protein expression level and graphical representations determined by Western blot analysis in DLD-1 and SW480 cells. (c) Cell growth determined by the CCK-8 assay. (d) Clonogenic assay of DLD-1 and SW480 cells. (e–f) The migration and invasion assay in DLD-1 and SW480 cells. (g) The real-time cell migration and invasion rates of DLD-1 and SW480 cells detected by RTCA DP analyzer. CADM2-OE: CADM2-Over-expression.

primary focal than adjacent normal tissue and further reduced in metastatic compared with primary focal. However, the mechanisms behind each of these steps remain unclear. Over the past decade, an increasing number of scholars have recognized the critical and complex role of the EMT process in promoting tumor invasion and metastasis. This process is controlled by different families of transcriptional regulators through

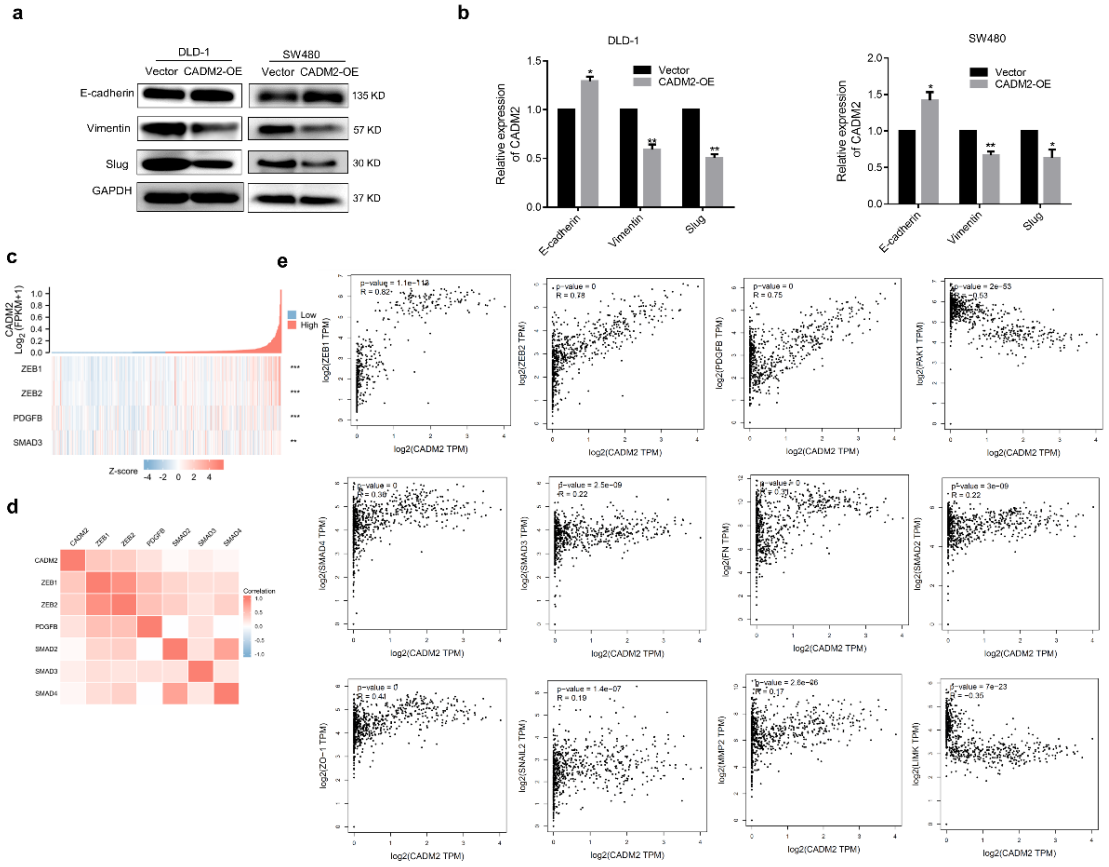

Fig. 4 CADM2 inhibiting epithelial-mesenchymal transition (EMT) process. (a) The expression of proteins related to the EMT process detected by Western blot analysis in DLD-1 and SW480 cells. (b) Graphical representations of the protein intensity levels. (c) Heatmap of single gene co-expression. (d) Heatmap of correlation between CADM2 and proteins related to the EMT process. (e) The scatterplot between CADM2 and proteins of the EMT process. CADM2-OE: CADM2-Over-expression.

distinct signaling pathways [34, 35]. In our study, we found that CADM2 up-regulation may inhibit the progression of CRC cells through the EMT process.

Tumor-infiltrating lymphocytes [36–38] in CRC have been shown to inhibit tumor growth and are associated with improved prognosis. Recent studies have found that individuals with a high density of infiltrating and effervescent memory T cells are less likely to have CRCs spread to lymphatic vessels and perineuronal structures as well as regional lymph nodes [36]. Research has shown that cell adhesion molecules and inflammatory cytokines can communicate with infiltrating immune stromal cells and tumor-associated stromal cells, promoting tumor growth, angiogenesis, metastasis, and immune suppression [39]. Similarly, we found a higher degree of immune cell infiltration and a higher enrichment score in the CADM2 high-expression subgroup.

Of course, there are still some shortcomings and deficiencies in this study. Since the correlation between CADM2 expression levels and clinicopathological features was not statistically significant, this part of the results was not presented. Besides, the exploration of the mechanism of metastasis is not deep enough.

Overall, we found that CADM2 was lowly expressed in primary cancer and further decreased in metastatic lesions. It can significantly distinguish normal tissue based on its mRNA expression level, suggesting that it can be used as a biomarker for the prognosis of CRC. Up-regulation of CADM2 inhibits the growth, migration, and invasion of CRC cells and attenuates metastasis by inhibiting the EMT process. This may provide insights for further exploration of the molecular mechanism of CRC metastasis.

Appendix A. Supplementary data

Supplementary data associated with this article can be found at http://dx.doi.org/10.2306/scienceasia1513-1874.2024.070. Data relevant to this study are available from the corresponding authors upon reasonable request.

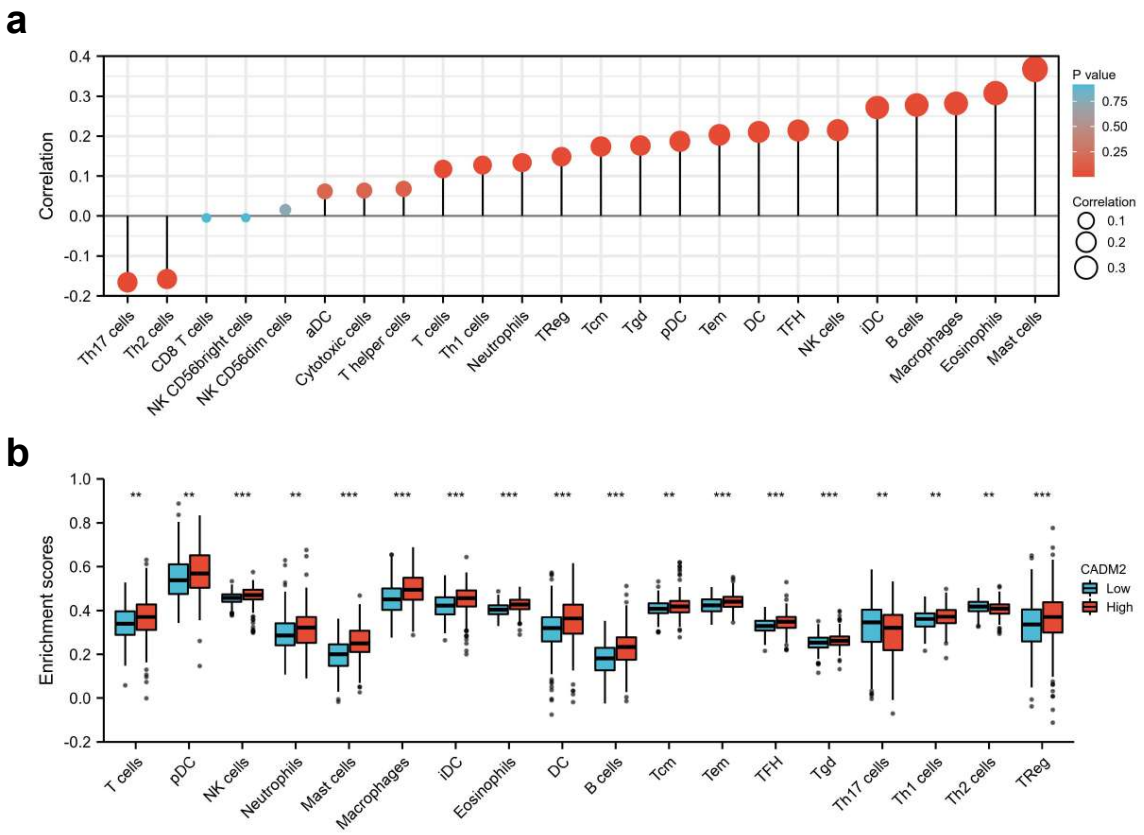

Fig. 5 Correlation between the expression level of CADM2 and immune infiltration in the tumor microenvironment. (a) Forest plot showing the correlation between the expression level of CADM2 and 24 immune cells. (b) Enrichment scores of 24 immune cells in different expression subgroups of CADM2. aDC: activated dendritic cells; iDC: immature dendritic cells; pDC: Plasmacytoid dendritic cells; Th: T helper cells; Tcm: T central memory; Tem: T effector memory; TFH: T follicular helper; and Tgd: T gamma delta.

Acknowledgements: This work was supported by the Wenzhou Municipal Science and Technology Bureau of China (Y20210742), the Zhejiang Provincial Natural Science Foundation of China (LQ22H200003 and LY24H160024), the Medical and Health Science and Technology Program of Zhejiang Province (2024KY1243), the Fundamental Scientific Research Fees of Wenzhou Medical University (KYYW2021026) and the National Natural Science Foundation of China (82272652).

REFERENCES

1. Siegel RL, Miller KD, Wagle NS, Jemal A (2023) Cancer statistics, 2023. *CA Cancer J Clin* **73**, 17–48.
2. Beech C, Hechtman J (2021) Molecular approach to colorectal carcinoma: Current evidence and clinical application. *Surg Pathol Clin* **14**, 429–441.
3. Bhullar DS, Barriuso J, Mullamitha S, Saunders MP, O'Dwyer ST, Aziz O (2019) Biomarker concordance between primary colorectal cancer and its metastases. *EBioMedicine* **40**, 363–374.
4. Piawah S, Venook AP (2019) Targeted therapy for colorectal cancer metastases: A review of current methods of molecularly targeted therapy and the use of tumor biomarkers in the treatment of metastatic colorectal cancer. *Cancer* **125**, 4139–4147.
5. Yang D, Hui Y, Bai S, Liang W, Hou J, Jiang J (2022) DUB3 contributes to colorectal cancer cell migration and angiogenesis via NF-κB/HIF-1α. *ScienceAsia* **48**, 359–366.
6. Dmello RS, To SQ, Chand AL (2021) Therapeutic targeting of the tumour microenvironment in metastatic colorectal cancer. *Int J Mol Sci* **22**, 2067.
7. Cheng Y, Fang X, Hu H, Wang J, Sun L, Yuan Y (2020) Successful treatment of metastatic colorectal cancer with synchronous *BRAF V600E* mutation and dMMR with BGB-A317. *Immunotherapy* **12**, 229–234.
8. Li Z, Xie Q, Wang B, Yu D, Liu C, Wang K, Zhang L, Zhu C (2023) A novel long noncoding RNA, AC005062.1, acts as an oncogene in colorectal cancer cell by regulating MACC1. *ScienceAsia* **49**, 595–602.
9. Gumbiner B (1996) Cell adhesion: the molecular basis of tissue architecture and morphogenesis. *Cell* **84**, 345–357.
10. Chang G, Xu S, Dhir R, Chandran U, O'Keefe DS, Greenberg NM, Gingrich JR (2010) Hypoexpression and epigenetic regulation of candidate tumor suppressor gene CADM-2 in human prostate cancer. *Clin Cancer Res* **16**,

5390–5401.
11. Chothia C, Jones E (1997) The molecular structure of cell adhesion molecules. *Annu Rev Biochem* **66**, 823–862.
12. Morris J, Bailey MES, Baldassarre D, Cullen B, de Faire U, Ferguson A, Gigante B, Giral P, et al (2019) Genetic variation in CADM2 as a link between psychological traits and obesity. *Sci Rep* **9**, 7339.
13. Greenbaum L, Ravona-Springer R, Livny A, Shelly S, Sharvit-Ginon I, Ganmore I, Alkelai A, Heymann A, et al (2019) The CADM2 gene is associated with processing speed performance – evidence among elderly with type 2 diabetes. *World J Biol Psychiatry* **20**, 577–583.
14. Hiruma A, Ikeda S, Terui T, Ozawa M, Hashimoto T, Yasumoto S, Nakayama J, Kubota Y, et al (2011) A novel splicing variant of CADM2 as a protective transcript of psoriasis. *Biochem Biophys Res Commun* **412**, 626–632.
15. Cao Z, Li S, Liu H, Li W, Sun Y, Li Z, Jia M, Su M (2021) The UFSP2/UFMylation pathway is involved in silica-induced pulmonary injury. *DNA Cell Biol* **40**, 589–594.
16. Liu Y, Li Y, Ren Z, Si W, Li Y, Wei G, Zhao W, Zhou J, et al (2017) MicroRNA-125a-3p is involved in early behavioral disorders in stroke-afflicted rats through the regulation of Cadm2. *Int J Mol Med* **40**, 1851–1859.
17. Yang S, Yan HL, Tao QF, Yuan SX, Tang GN, Yang Y, Wang LL, Zhang YL, et al (2014) Low CADM2 expression predicts high recurrence risk of hepatocellular carcinoma patients after hepatectomy. *J Cancer Res Clin Oncol* **140**, 109–116.
18. Yang L, Zhao G, Wang F, Li C, Wang X (2018) Hypoxia-regulated miR-146a targets cell adhesion molecule 2 to promote proliferation, migration, and invasion of clear cell renal cell carcinoma. *Cell Physiol Biochem* **49**, 920–931.
19. Huang YX, Nie XG, Li GD, Fan DS, Song LL, Zhang XL (2018) Downregulation of microRNA182 inhibits cell viability, invasion and angiogenesis in retinoblastoma through inhibition of the PI3K/AKT pathway and CADM2 upregulation. *Int J Oncol* **53**, 2615–2626.
20. Wang Y, Zhao J, Wang Y, Gao J, Yang H, Li H (2022) MiR-17-5p targets and downregulates CADM2, activating the malignant phenotypes of colon cancer cells. *Mol Biotechnol* **64**, 1388–1400.
21. Picard E, Verschoor CP, Ma GW, Pawelec G (2020) Relationships between immune landscapes, genetic subtypes and responses to immunotherapy in colorectal cancer. *Front Immunol* **11**, 369.
22. Galon J, Costes A, Sanchez-Cabo F, Kirilovsky A, Mlecnik B, Lagorce-Pagès C, Tosolini M, Camus M, et al (2006) Type, density, and location of immune cells within human colorectal tumors predict clinical outcome. *Science* **313**, 1960–1964.
23. Angelova M, Charoentong P, Hackl H, Fischer ML, Snajder R, Krogsdam AM, Waldner MJ, Bindea G, et al (2015) Characterization of the immunophenotypes and antigenomes of colorectal cancers reveals distinct tumor escape mechanisms and novel targets for immunotherapy. *Genome Biol* **16**, 64.
24. Lu F, Fang D, Li S, Zhong Z, Jiang X, Qi Q, Liu Y, Zhang W, et al (2022) Thioredoxin 1 supports colorectal cancer cell survival and promotes migration and invasion under glucose deprivation through interaction with G6PD. *Int J Biol Sci* **18**, 5539–5553.
25. Bindea G, Mlecnik B, Tosolini M, Kirilovsky A, Waldner M, Obenauf AC, Angell H, Fredriksen T, et al (2013) Spatiotemporal dynamics of intratumoral immune cells reveal the immune landscape in human cancer. *Immunity* **39**, 782–795.
26. Schulz W (1998) DNA methylation in urological malignancies (review). *Int J Oncol* **13**, 151–167.
27. Li X, Chen D, Li M, Gao X, Shi G, Zhao H (2018) The CADM2/Akt pathway is involved in the inhibitory effect of miR-21-5p downregulation on proliferation and apoptosis in esophageal squamous cell carcinoma cells. *Chem Biol Interact* **288**, 76–82.
28. He W, Li X, Xu S, Ai J, Gong Y, Gregg JL, Guan R, Qiu W, et al (2013) Aberrant methylation and loss of CADM2 tumor suppressor expression is associated with human renal cell carcinoma tumor progression. *Biochem Biophys Res Commun* **435**, 526–532.
29. Dai L, Li YH, Liang YY, Zhao J, Chen G, Yin J, Postmus PE, Addeo A, et al (2021) High expression of cell adhesion molecule 2 unfavorably impacts survival in non-small cell lung cancer patients with brain metastases. *J Thorac Dis* **13**, 2437–2446.
30. Kang GH, Lee S, Lee HJ, Hwang KS (2004) Aberrant CpG island hypermethylation of multiple genes in prostate cancer and prostatic intraepithelial neoplasia. *J Pathol* **202**, 233–240.
31. Lou W, Krill D, Dhir R, Becich MJ, Dong JT, Frierson HF Jr, Isaacs WB, Isaacs JT, et al (1999) Methylation of the CD44 metastasis suppressor gene in human prostate cancer. *Cancer Res* **59**, 2329–2331.
32. Li LC, Zhao H, Nakajima K, Oh BR, Ribeiro Filho LA, Carroll P, Dahiya R (2001) Methylation of the E-cadherin gene promoter correlates with progression of prostate cancer. *J Urol* **166**, 705–709.
33. Asayut S, Puttipanyalears C, Rattanatanyong P, Thanasitthichai S, Kitkumthorn N, Mutirangura A (2021) RHEB methylation in white blood cell, a novel candidate marker for breast cancer screening. *ScienceAsia* **47**, 143–152.
34. Zhang N, Ng AS, Cai S, Li Q, Yang L, Kerr D (2021) Novel therapeutic strategies: targeting epithelial-mesenchymal transition in colorectal cancer. *Lancet Oncol* **22**, e358–e368.
35. Manfioletti G, Fedele M (2023) Epithelial-mesenchymal transition (EMT). *Int J Mol Sci* **24**, 11386.
36. Pagès F, Berger A, Camus M, Sanchez-Cabo F, Costes A, Molidor R, Mlecnik B, Kirilovsky A, et al (2005) Effector memory T cells, early metastasis, and survival in colorectal cancer. *N Engl J Med* **353**, 2654–2666.
37. Baier PK, Wimmenauer S, Hirsch T, von Specht BU, von Kleist S, Keller H, Farthmann EH (1998) Analysis of the T cell receptor variability of tumor-infiltrating lymphocytes in colorectal carcinomas. *Tumour Biol* **19**, 205–212.
38. Diederichsen AC, Hjelmborg J, Christensen PB, Zeuthen J, Fenger C (2003) Prognostic value of the CD4+/CD8+ ratio of tumour infiltrating lymphocytes in colorectal cancer and HLA-DR expression on tumour cells. *Cancer Immunol Immunother* **52**, 423–428.
39. Huang HW, Chang CC, Wang CS, Lin KH (2021) Association between inflammation and function of cell adhesion molecules influence on gastrointestinal cancer development. *Cells* **10**, 67.

Appendix A. Supplementary data

Table S1 Primer sequence.

Primer	Sequence (5′–3′)
CADM2-F (qPCR)	GTGCATGATGTTCCCAACACT
CADM2-R (qPCR)	TGTGGTTGGGCTGGTTGTTATG
CADM2-F (MSP)	TTTTGCGGGTGTTTTGTC
CADM2-R (MSP)	TAATATCCTCCTCCCGACG
GAPDH-F	TTCATTGACCTCAACTACATGGTTTAC
GAPDH-R	TGACAAGCTTCCCGTTCTCA

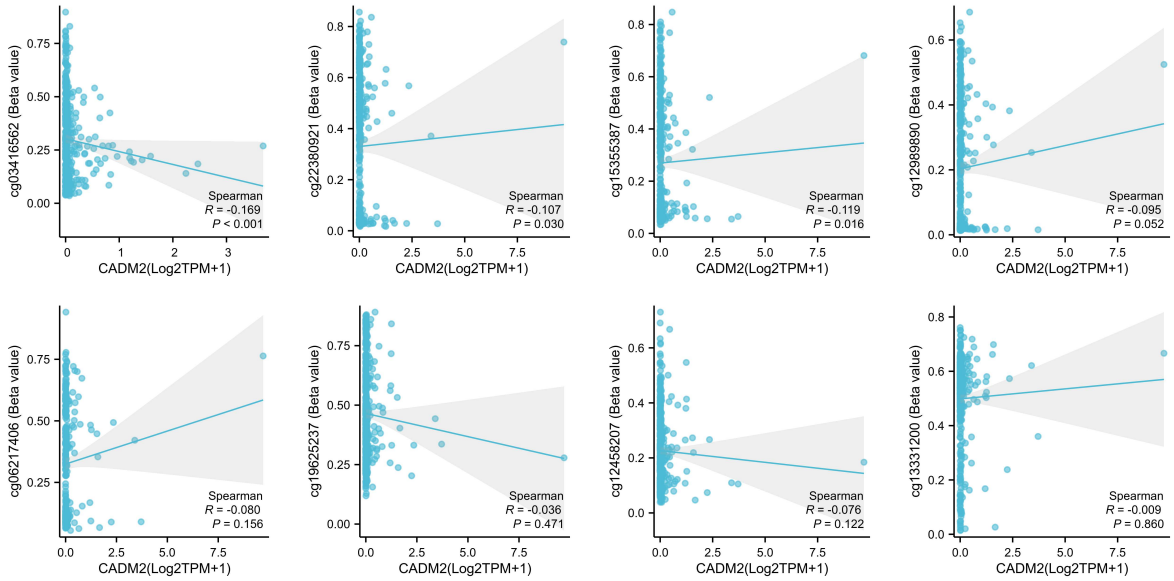

Fig. S1 Scatterplot of correlation between CADM2 expression level and methylation level of promoter region.